Grafting of Bioactive Polymers with Various Architectures: A Versatile Tool for Preparing Antibacterial Infection and Biocompatible Surfaces

Hamza Chouirfa, Margaret Evans, Penny Bean, Azzam Saleh-Mghir, Anne Claude Crémieux, David Castner, Céline Falentin-Daudré, Véronique Migonney

HHS Public Access

Author manuscript

ACS Appl Mater Interfaces. Author manuscript; available in PMC 2019 January 17.

Published in final edited form as:

ACS Appl Mater Interfaces. 2018 January 17; 10(2): 1480–1491. doi:10.1021/acsami.7b14283.

Grafting of bioactive polymers with various architectures: a versatile tool for preparing antibacterial infection and biocompatible surfaces

Hamza Chouirfa[1], **Margaret D. M. Evans**[2], **Penny Bean**[2], **Azzam Saleh-Mghir**[3], **Anne Claude Crémieux**[3], **David G. Castner**[4], **Céline Falentin-Daudré**[1], and **Véronique Migonney**[1,*]

[1]LBPS/CSPBAT, UMR CNRS 7244, Institut Galilée, Université Paris 13, Sorbonne Paris Cité, 99 avenue JB Clément, 93340 Villetaneuse, France

[2]CSIRO Biomedical Materials Manufacturing Program, 11 Julius Avenue, North Ryde, Sydney, NSW 2113, Australia

[3]Département de Médecine Aigüe Spécialisée, Hôpital Universitaire Raymond-Poincaré, Assistance Publique - Hôpitaux de Paris, Garches, and UMR 1173, Faculté de Médecine Paris-Île-de-France Ouest, Université Versailles-Saint-Quentin, Versailles, France

[4]National ESCA and Surface Analysis Center for Biomedical Problems, Departments of Bioengineering and Chemical Engineering, University of Washington, Seattle, Washington 98195-1653

Abstract

The aim of this article is to present three different techniques of poly(sodium styrene sulfonate) (polyNaSS) covalent grafting onto titanium (Ti) surfaces and study the influence of their architecture on biological response. Two of them are “grafting from” techniques requiring an activation step either by thermal or UV irradiation. The third method is a “grafting to” technique involving an anchorage molecule onto which polyNaSS synthesized by Reversible Addition-Fragmentation Chain Transfer (RAFT) polymerization is clicked. The advantage of the “grafting to” technique when compared to the “grafting from” technique is the ability to control the architecture and length of the grafted polymers on the Ti surface and their influence on the

[*]**Corresponding author**. veronique.migonney@univ-paris13.fr, LBPS/CSPBAT, UMR CNRS 7244, Institut Galilée, Université Paris 13 Sorbonne Paris Cité, 99 avenue JB Clément 93340-Villetaneuse, France.

Author contributions

Hamza Chouirfa as PhD student was in charge the following experiments: chemistry, physicochemistry (FTIR, SEM-EDX, BT, contact angle), protein adsorption and bacteria adhesion. Except for the bacteria adhesion assays, the experiments were achieved at the LBPS/CSPBAT UMR CNRS 7244, University Paris 13, Villetaneuse, France.

Margaret D. M. Evans and Penny Bean were in charge of the cell response study: cell culture, imaging and analysis. All the experiments were achieved at the CSIRO, Sydney, Australia.

Azzam Saleh-Mghir and Anne Claude Crémieux as experts in bacterial adhesion initiated Hamza Chouirfa and allowed him to carry out the bacterial adhesion assays at the Hôpital Universitaire Raymond-Poincaré, Garches, France.

David G. Castner was in charge of all the XPS characterization experiments and analyses achieved at the NESAC/BIO UW, Seattle, USA.

Céline Falentin-Daudré initiated Hamza Chouirfa to the synthesis of the DOPA derivatives and of the polymer synthesis by RAFT and to the grafting from and to processes.

Véronique Migonneyas supervisor of the PhD program of Hamza Chouirfa set up the study program and analyzed the whole results. The manuscript was written through contributions of all authors.

biological responses. This investigation compares the effect of the three different grafting processes on the *in vitro* biological responses of bacteria and osteoblasts. Overall outcomes of this investigation confirmed the significance of the sulfonate functional groups on the biological responses, regardless of the grafting method. In addition, results showed that the architecture and distribution of grafted polyNaSS on Ti surfaces alter the intensity of the bacteria response mediated by fibronectin.

Graphical abstract

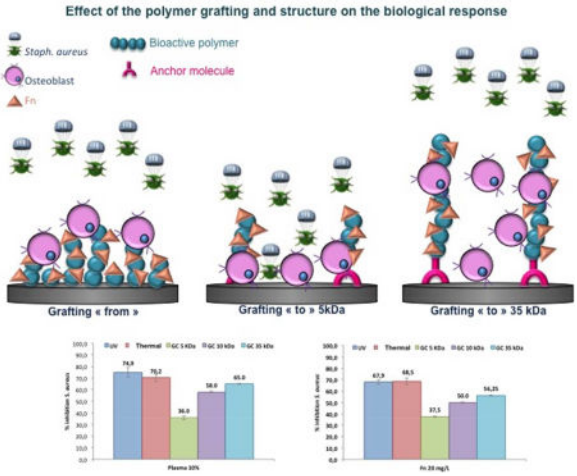

Keywords

grafting from; grafting to; polyNaSS; *S. aureus*; titanium

1. Introduction

Titanium (Ti) and its alloys are materials of choice for orthopaedic and dental implant applications as well as for fixation devices because of their biocompatibility and anti-corrosion properties, as well as mechanical properties, which are closer to those of bone than many other materials.[1–3]

Nevertheless, despite the considerable progresses made in materials science, surgical techniques and surface modification, the infection of implanted medical devices remains too high and is still a challenge to the durability and osteointegration of Ti implants.[4–8] Various strategies have been developed[9–12] to promote osseointegration of Ti surfaces, including modification of their topography and physicochemical properties, while only a few strategies have been proposed for prevention of the infection.[13–20] Insofar as prosthetic infection is a major public health issue, the development of bioactive Ti surfaces that can promote osseointegration while also controlling and/or preventing bacteria adhesion appears to be the best approach to improve the lifespan of the implants. Indeed, when one prosthesis is infected, the only way to stop the infection is often the removal of the implant.

The strategy of choice to prevent implant infection is the inhibition of bacteria adhesion, which is the first step of infection. Amongst the different bacterial strains detected in joint prosthesis infections, the most common remain *Staphylococcus aureus* (*S. aureus*) and *Staphylococcus epidermidis (S. epi)*, with both staphylococcus strains having strong affinities to metallic surfaces such as Ti.[21] The strategies used to date for overcoming Ti implant-related infection are limited for the following reasons: (i) the systematic prophylactic use of antibiotics in the clinic may induce the development of bacteria strains resistant to antibiotics, (ii) the removal of the implant is typically required when infection is proven to present, and (iii) antibiotic mixtures are required to contain the infection. As the massive use of antibiotics presents the disadvantage of introducing antibiotic resistance, the surface modification and/or functionalization of Ti surfaces to reduce bacterial adhesion[22] is a promising solution. Various Ti surface modifications previously proposed include ion (Ag, Co) implantation,[23] plating (TiN, alumina), ion (Ag, Sn, Zn, Pt) beam mixing,[13] polycationic groups,[14,15] polyelectrolyte multilayers of acid hyaluronic, and chitosan.[16] When positive results are obtained *in vitro*, they are mainly focused on bacteria response and not addressing the cell and tissue response to the implants, which is inseparable part of biological response. In addition, the benefits of these treatments are not always demonstrated *in vivo*.

Our approach is different as it does not separate the cell and bacteria responses. We showed that poly(sodium styrene sulfonate) (polyNaSS) grafted surfaces enhance the *in vivo* osteoblast cell response (osseointegration) while inhibiting bacteria adhesion. The mechanism at the origin of these activities comes from the presence of carboxylate and sulfonate groups – glycosaminoglycan-like surfaces, which modulated the adsorption of binding proteins as fibronectin (Fn) and their conformation. These groups randomly distributed along the macromolecular chains of various poly(methyl methacrylate) (PMMA), poly(styrene) or poly(vinyl chloride) based copolymers have been demonstrated to promote specific interactions with selected adhesive proteins[24,25] such as fibronectin, which is known to mediate *S. aureus* adhesion.[17] In addition, when grafted on silicone matrices, sulfonate and carboxylate groups from polyNaSS and PMMA chains have been shown to modulate the inhibition of *S. aureus* adhesion *in vitro*[18,19] and *in vivo*.[20] Extensive studies described the mechanism on model copolymers exhibiting carboxylate and sulfonate anionic groups showed that varying the carboxylate/(carboxylate + sulfonate) ratio allowed modulating cell response and bacteria adhesion. In addition, several *in vitro* and *in vivo* studies have reported that sulfonate groups, when present at the surface of Ti and poly(ethylene terephtalate) implant surfaces, enhance adhesion, proliferation, and differentiation of osteoblasts that are the prerequisites to osseointegration.[26,27] The interest of the covalent grafting of polyNaSS on prosthetic surfaces is to offer a high stability of the coating *in vivo*: implantations performed in rabbits highlight the maintenance of biological activity up to 12 months. It is worthy noting that polyNaSS grafted THP have been selected and authorized to be tested in a clinical human trial.[28]

We decided to graft polyNaSS onto Ti implant surfaces because the presence of sulfonate groups gave the best compromise between the osteoblasts cell response and the inhibition of bacteria adhesion *in vitro* and *in vivo*.

Until now, we observed the biological responses of polyNaSS grafted surfaces by using the "grafting from", which didn't allow the influence of architecture, length and distribution of grafted polyNaSS macromolecular chains on the biological response to be properly addressed. This information is needed to propose a mechanism and/or a structure-properties relationship between polyNaSS surface chemistry and biological response.

The present study investigated the effect of different architecture and distribution of polyNaSS grafted macromolecules onto Ti surfaces on the *in vitro* osteoblast cell response and *S. aureus* adhesion. To achieve this goal we carried out three different way of grafting polyNaSS onto Ti surfaces:

- the "grafting from" technique involving the activation of the surface by oxidation and thermal activation was used as a reference and internal control for all the *in vitro* and *in vivo* results.
- the "grafting from" technique involving the activation of the surface by oxidation and UV activation
- the "grafting to" technique using an anchorage molecule to which polyNaSS chains of various lengths synthesized by RAFT polymerization are clicked onto.

The three different polyNaSS grafted surfaces were then exposed to cell and bacteria in order to eludate the effect of the architecture and distribution of sulfonate groups on the inhibition properties of *S. aureus* adhesion as well the osteoblast behavior.

2. Materials and Methods

2.1. Materials

One-centimeter diameter Ti (Grade 2) disks were obtained from GoodFellow. The two faces of the disks were polished consecutively with 500 and 1200 grit SiC papers for ≈2–3 min each. After polishing, the surfaces were cleaned in acetone overnight under stirring. The following day, the surfaces were cleaned once in an acetone bath and then three times in distilled water (dH_2O) bath with sonication for 15 min. Then, the disks were put in Kroll's reagent (2% HF, Sigma; 10% HNO_3, Acros and 88% dH_2O) for one minute with stirring followed by 15 min sonication treatments in five consecutive dH_2O baths. Sodium styrene sulfonate (NaSS monomer, Sigma) was purified by recrystallization in a mixture of water/ethanol (10/90 *v/v*), dried at 50°C under vacuum, and then stored at 4°C.

2.2. Methods

PolyNaSS chemical grafting was performed using both "grafting from" and "grafting to" techniques. The "grafting from" process included the thermal and UV grafting, as described by Hélary et *al.*[29] and Chouirfa et *al.*,[30,31] respectively. The UV grafting is 15 times faster than the thermal grafting and uses half as much monomer (0.32 M for UV grafting vs. 0.7 M for thermal grafting). The "grafting to" procedure was described in detail by Chouirfa et *al.*[32] The main difference between the "grafting from" and the "grafting to" technique is the architecture of the grafted polymers and the homogeneity of polymer grafted covering of the surface (Scheme 1). The "grafting from" uses radical polymerization and generates grafted

polymers with a range of molecular weights, but with good surface coverage. In fact the length of grafted from polymers chains is low (DPn 5 to 10). In the case of the “grafting to” technique, the grafted polymers on the titanium surface have been polymerized by RAFT synthesis, which result in a controlled architecture and well defined molecular weight (5, 10 and 35 kDa), but the surface coverage is lower than in the case of the “grafting from” process. Overall, three grafted surfaces were prepared and compared to a control Ti surface that was not polyNaSS grafted as detailed in Table 1.

The grafted polyNaSS Ti surface produced *via* the “grafting to” process needs the incorporation of an anchoring molecule (catechol derivative) to attach the polyNaSS chains onto the Ti surface. In Figure 1, the polyNaSS structure is represented differently according the grafting method used (“grafting from” or “grafting to”).

2.3. Characterization

The presence of poly(NaSS) chains on the grafted surfaces was determined using the toluidine blue (TB) colorimetric method,[30] Fourier-transformed infrared (FTIR),[30,32] X-ray photoelectron spectroscopy (XPS),[31] contact angle,[30] quartz crystal microbalance with dissipation (QCM-D).[32]

For the TB analysis, Ti disks were individually immersed in a TB (Acros) aqueous solution (5×10^{-4} M) at 30°C for 6 hrs, allowing TB complexation with SO_3^- groups from poly(NaSS).[33,34] Surfaces were incubated with 5×10^{-3} M aqueous sodium hydroxide solutions to remove the non-complexed dye. Disks were then immersed in a mixture of acetic acid/dH_2O (50/50 *v/v*, Sigma) for 24 hrs, inducing TB decomplexation. The concentration of the decomplexed TB was measured by visible spectroscopy at 633 nm using a Perkin-Elmer spectrometer lambda 25.

Static solvent contact angles were measured using a DSA10 contact angle measuring system from KRUSS GmbH. A droplet of solvent was suspended from the tip of a microliter syringe supported above the sample stage. The image of the droplet was captured and the contact angle was measured using DSA drop shape analysis program from KRUSS. The contact angle of distilled water (2 μL) on the surface was recorded 10 s after contact. Three measurements were taken and averaged for each sample.

XPS data were acquired on a Surface Science Instruments S-probe spectrometer. This instrument has a monochromatized Al Kα X-ray and a low energy electron flood gun for charge neutralization of non-conducting samples. The samples were mechanically fastened to the sample holder and run as conductors. X-ray spot size for these acquisitions was approximately 800 μm. Pressure in the analytical chamber during spectral acquisition was less than 5×10^{-9} torr. Analyzer pass energy for the survey and detail scans was 150 eV. The photoelectron take-off angle (the angle between the sample normal and the input axis of the energy analyzer) was 0°, which corresponds to a ≈10 nm sampling depth. Service Physics Hawk Data Analysis 7 Software was used calculate surface atomic concentrations using peak areas above a linear background from the survey and detail scans and elemental sensitivity factors. Three spots were analyzed from each replicate. Each analysis spot included a survey spectrum and detail spectra for the Na1s and S2p peaks.

2.4. Cell culture

Preparation of titanium surfaces—Prior to cell culture, ungrafted and grafted Ti surfaces substrates were extensively washed with saline aqueous solutions: 1.5 M sodium chloride (NaCl, Fisher), 0.15 M NaCl, pure water and phosphate buffered saline solution (PBS, Gibco), each step was repeated three times. The surfaces were finally air dried and sterilized on both sides by exposure to ultraviolet light (UV, 30 W) for 15 min.

Cell assays

a) initial adhesion assay: Saos-2 cells (purchased from ATCC, USA) were seeded onto sterilized Ti surfaces held individual wells of 24-well TCPS plate at a density of $1.5\times10^4/cm^2$ in standard culture medium. TCPS wells were established as internal controls for the assay. Plates were routinely incubated at 37°C in a humidified atmosphere containing 5% CO_2 in air and allowed to adhere and spread to 2 time-points of 24h and 48h at which point medium was removed and samples rinsed twice with PBS, fixed for 30 min at rt in 4% paraformaldehyde in PBS, washed 2× with PBS, and cells immunostained with anti-tubulin antibody to visualize cells on opaque surfaces. Prior to immunostaining, cells were permeabilized with 0.1% Triton X-100 (Sigma-Aldrich) in PBS for 5', washed twice with PBS, then blocked for 1h in 1% BSA/PBS. Blocking buffer was replaced with alpha-tubulin antibody (ThermoFisher Scientific, Australia A11126) diluted 1/200 in blocking buffer and incubated overnight at 4°C. Samples were brought to room temperature, washed 3× with blocking buffer and incubated for 90' in FITC conjugated rabbit anti-mouse immunoglobulins (Dako F0261) diluted 1/20 in blocking buffer. Samples were washed twice in PBS, counterstained with DAPI diluted 1/1000 for 5' at rt, washed twice more with PBS before viewing using a confocal microscope (Nikon Eclipse Ti) with images collected using a digital camera.

b) proliferation assay: Saos-2 cells were seeded onto grafted and ungrafted Ti surfaces (in triplicate) held in 24-well TCPS plates at a density of $1.5\times10^4/cm^2$ in standard culture medium and incubated at 37°C with 5% CO_2 in air to timepoints of days 1, 4 and 7 with triplicate samples of each Ti surface and control TCPS. The number of adherent cells was measured in triplicate wells at days 1, 4 and 7 using a routine MTT assay and morphology of cells on surfaces examined in fourth well on day 7. Cell morphology was examined by staining cells adherent to wafers with 1/1000 dilution of Cell Tracker Green CFMDA dye (CTG, from ThermoFisher Scientific) for 60 minutes. Stained cells were then fixed in 4% formal saline and examined using an inverted fluorescent microscope at wavelength of 488nm (Nikon Eclipse Ti).

(iii) cell differentiation and mineralization

Cell culture for differentiation/mineralization: Sterilized samples of each of the Ti surfaces were placed into individual wells of 24-well plates and seeded with Saos-2 cells at a concentration of 3×10^4 cells/cm^2 in standard culture medium and incubated undisturbed for 4 days. At that time, culture medium in one series of plates was replaced with the standard culture medium (*standard control series*) and in the other set with osteogenic differentiation medium comprised by DMEM/Hams F12 containing the standard supplements in addition to

osteogenic supplements of β-Glycerophosphate (BGP) at 1.5 mg/mL (7mM), Dexamethasone (Dex) at 40 ng/mL (100mM), and Ascorbic acid (Asc) at 20 μg/mL (70μM) all sourced from Sigma-Aldrich (*osteogenic series*). Differentiation was determined by measuring the production of both alkaline phosphatase and calcium in the adherent cells under both of the standard and osteogenic culture regimes. A representative sample of each treatment was also stained with Cell Tracker Green on completion for visualization of cell cover on the opaque surfaces.

Cell proliferation: was measured on cells on all surfaces maintained in standard and osteogenic conditions at day 25 using a routine MTT assay. All MTT results were adjusted for differences in areas of wafers/wells and normalized to values for cells grown in TCPS control wells under undifferentiated and differentiated culture regimes. This enabled the differentiation/mineralization data (alkaline phosphatase and calcium) to be adjusted according to the number of cells attached to each substrate and TCPS controls at day 25 (as described below).

Cell coverage was examined on one representative wafer per set at day 25 using Cell Tracker Green to enable visualization of cell coverage on each type of Ti wafer.

Cytotoxicity check was performed by taking phase contrast images of the cells attached to the TCPS wells around each wafer prior to performing the MTT assay associated with the differentiation/mineralization assay.

Differentiation and mineralization of cells: was evaluated by measuring the production of calcium and alkaline phosphatase by cells adherent to each type of Ti wafer in both the standard and osteogenic culture regimes at day 25 (as detailed below).

Alkaline Phosphatase: was measured in cells adherent to the substrates at 25 days using a quantitative assay based on p-nitrophenyl phosphate (p-NPP from Sigma-Aldrich N1891). 500μl of p-NPP at a concentration of 2.0 mg/ml in 0.1M glycine buffer was added to each well containing a Ti wafer and shaken at 37°C for 60’ then the reaction was neutralized by the addition of 500μl 1M NaOH per well. The optical density of wells containing test samples, controls and standards was read using a spectrophotometer set on wavelength of 405nm (Molecular Devices Spectramax). Sample sets were compared to a standard curve prepared from 10μM/ml stock solution of p-NPP diluted in 0.1M glycine buffer and neutralized to create 8 standards ranging from p-NPP dilutions of 1/5 to 1/640.

Calcium: was evaluated using a calcium sensitive dye, Arsenazo III, in a quantitative assay to determine the amount of calcium produced by cells adherent to each substrate after 25 days in culture. Each Ti wafer was transferred to a fresh well and 500 μl 0.6M HCl added then plates shaken at rt overnight to permeabilize cells and release the calcium. The reaction was neutralized the next day by the addition of 100μl 3M NaOH per well. A 20μl aliquot was taken from each well and mixed with 200μl of Arsenazo III reagent (Sigma#11090) at a concentration of 0.15mg/ml to form a complex with the calcium which resulted in a color change. The optical density of the test samples, controls and standards wells was read on a spectrophotometer set on a wavelength of 595nm (Molecular Devices Spectramax). Sample

sets were compared to a standard curve prepared from 1mg/ml $CaCl_2$ stock solution diluted in H_2O to create 8 standards ranging from $CaCl_2$ dilutions of 1/100 to 0 μg/ml.

For both ALP and calcium assays: the resulting values were adjusted to take in account the differences in sample areas between all Ti wafers (0.8 cm^2) and the control TCPS wells (2 cm^2) with final values expressed as either p-NPP mM/cm^2 or calcium mg/cm^2. Data were then normalized to the value of the TCPS control in osteogenic culture regime to give a percentage value and then corrected to take into account the number of cells present on surfaces as determined by the MTT assay run in parallel over the 25 day period.

2.5. Bacteria adhesion

Clinical meticillin resitant strain *S. aureus* MRSA 88244 was provided by Prof. A. C. Crémieux, Hôpital Raymond Poincaré, Garches, France. The bacterial strain was stored at −80°C in Brain Heart Infusion (BHI) broth (Bio-Rad Laboratories). The bacteria were initially thawed; spread in a Muller Hinton Agar (Bio-Rad Laboratories) gel and incubated for 18 h at 37°C. For each experiment, one colony of *S. aureus* was extracted and combined with 9 mL of Trypto-Casein-Soja (TCS) (Bio-Rad Laboratories) to expand overnight at 37°C. The adhesion of *S. aureus* (88244) onto poly(NaSS) grafted and ungrafted Ti was assessed following the experimental procedure derived from Felgueiras et *al.*[26]

The effect of preadsorbing proteins onto Ti samples was also investigated. Albumin passivation was done by incubating the samples with 0.4 g/L human serum albumin (HSA) PBS solutions for 30 min at 37°C under stirring to avoid non-specific adsorption. Pure or mixed proteins adsorbed for 1 h at 37°C under stirring included HSA, platelet poor plasma (PPP, 10% plasma), Fibronectin (Fn) and depleted platelet poor plasma (dPPP) not supplemented with Fn.

Prior to any bacteria experiment, the growth parameters for bacteria proliferation were established and the corresponding exponential phase identified (phase when bacteria exhibit the highest adhesin expression).

One colony was suspended in fresh 9 mL of TCS medium and its absorbance was measured in duplicate at 600 nm. Two suspensions were then prepared and incubated at 37°C. Their absorbance was read every 30 min. The bacterial exponential phase was determined to occur at 4 hrs. Thus, 3 hrs was the time selected for bacterial culture prior to seeding. The colony expanded overnight was centrifuged and re-suspended in 1 mL of physiological water (0.85%). 160 μL of the previous were then combined with 1 mL of Trypto-Caseine-Soja (TCS) and incubated for 3 hrs at 37 °C. The bacterial solution was centrifuged, the supernatant discarded, and 20 mL of PBS was added. The bacterial suspension was then prepared with a concentration of approximately 10^6 CFU/mL. 1 mL of this solution was added to each sample, which included ungrafted and grafted surfaces adsorbed with PPP, dPPP, HSA (4 g/L) (Sigma), Fn (20 mg/L) (Sigma), dPPP + Fn (20 mg/L) and incubated for 1 h. After 1 hr the bacteria were detached using trypsin to determine their number. Data were reported as a function of the initial seeding number. The inhibition of bacterial adhesion exhibited by poly(NaSS) grafted Ti samples was expressed as a percentage of the bacteria adhesion obtained on ungrafted Ti samples, which was considered to be 100%.

Bacteria attached to ungrafted and grafted Ti surfaces pre-adsorbed with pure plasma for 1 h were stained with 1/1000 (*v/v*) propidium iodide in PBS for 5 min. The surfaces were then carefully washed with PBS, protected from light and observed by fluorescent microscopy.

3. Results and Discussions

3.1. Surface characterization

The polyNaSS grafted surfaces prepared using the thermal and UV "grafting from" methods were characterized by ATR-FTIR, TB, contact angle and XPS as described by Felgueiras, Hélary and Chouirfa *et al.*[29–31] The polyNaSS with different molecular weights (5, 10 and 35 kDa) synthesized by RAFT and grafted using the "grafting to" method were characterized by QCM-D, angle contact, TB, XPS, ATR-FTIR as described by Chouirfa *et al.*[32] In this study we focused the analysis of the distribution of the grafted poly NaSS chains across the Ti surfaces comparing contact angle, TB, and XPS results.

The XPS results in Table 2 show the C, Ti, O, N, S and Na surface concentrations for the different grafted films. For each sample, we find the characteristic elements of polyNaSS, both for the "grafting from" samples (Ti-TH and Ti-UV) and for the "grafting to" samples (Ti-PR ≈5, 10, 35 kDa). The highest S concentration (≈7 atomic %), an element characteristic of the polyNaSS overlayer, along with lowest Ti concentration (≈2.5 atomic %), an element characteristic of the Ti substrate, were detected on the Ti-TH and Ti-UV samples. This indicates the Ti-TH and Ti-UV samples had a thicker and/or denser polyNaSS overlayer compared to the Ti-PR samples. Within the Ti-PR samples, the 5 and 10 kDa samples had the lowest S concentrations (≈2.5 atomic %) and highest Ti concentrations (≈7 atomic %). The Ti-PR 35 kDa sample had S and Ti concentrations that approached the concentrations observed for the Ti-TH and Ti-UV samples.

When titanium surface is covered by a hydrophilic polymer, the contact angle formed by a water droplet is decreased. PolyNaSS being an anionic and hydrophilic polymer, when grafted on the Ti surface should lead to a lower contact angle when compared to the ungrafted Ti surface. According to Figure 2, the presence of polyNaSS on the grafted titanium surfaces leads to contact angles lower than that of the Ti control (≈108°): the "grafting from" technique used for the Ti-TH and Ti-UV surfaces results in contact angle values (θ) of ≈15° and ≈16°, respectively, which are ≈3× lower than the θ observed for the "grafting to" surfaces Ti-PR 5 (≈50°), 10 (≈52°) and 35 (≈53°) kDa. The contact angle measurements showed that regardless of the activation method (thermal or UV) the "grafting from" methods produced similar surfaces. The significantly lower contact angles observed for the "grafting from" methods compared to the "grafting to" method suggest a more complete covering of polyNaSS chains on Ti surfaces by using the "grafting from " methods, consistent with the higher sulfur contents observed by XPS for these samples.

The TB results for the different grafted surfaces were consistent with the contact angle and XPS results. As shown in Table 3 the amount of poly(NaSS) grafted is significantly higher on samples functionalized by the "grafting from" method compared to samples functionalized by the "grafting to" method (~5 μg/cm^2 vs. <1 μg/cm^2). XPS also showed more poly(NaSS) on the "grafted from" surfaces compared to the "grafted to" surfaces (~7

atomic % S compared to 2–5 atomic % S). Thus, the higher amounts of grafted poly(NaSS) combined with the lower contact angle values observed for the “grafted from” samples indicate the “grafting from” method results in more complete coverage of the Ti surface by polyNaSS macromolecular chains. The lower coverage obtained using the “grafting to” process is likely due to increased steric effects encountered when grafting long macromolecular chains, which makes it more difficult to pack the RAFT polymerized chains closely together compared to polymerizing monomers from the surface in the “grafting from” process.

Visually (Figure 3) the results of TB colorimetric assay are clearly different when comparing the “grafting from” to the “grafting to” samples. Assuming 1 mol of TB forms a complex with 1 mol of sulfonate groups, TB assay provides a macroscopic information about the distribution of the grafted polyNaSS on Ti surfaces. The photos clearly show that the “grafting from” technique compared to the “grafting to” technique gives a darker blue image due to the higher concentration of sulfonate groups on the « grafting from » surface.

3.2. Evaluation of the cell response

The aim of the cell response experiments was to compare 3 different grafting methodologies (Ti-UV, Ti-TH, Ti-PR) used to functionalize the surface of Ti samples with polyNaSS to each other as well as ungrafted Ti control samples to establish a structure/biological properties relationship. The biological response to all the Ti surfaces was evaluated using human bone-derived cell line Saos-2 in a series of *in vitro* cell-based assays to measure initial cell adhesion and spreading, cell proliferation and cell differentiation.

3.2.1. Initial cell adhesion (spreading and morphology)—The initial adhesion of cells onto ungrafted Ti and grafted Ti (Ti-UV, Ti-TH, Ti-PR) surfaces was examined after 24 hrs and 48 hrs of culture by staining the microtubules of the cell cytoskeleton with tubulin antibody and the nuclei with DAPI to visualize the cells (Figure 4). On both the grafted and ungrafted surfaces as well as the control tissue culture plastic control (Permanox), the cells had attached and were well spread by 24 hrs. At this timepoint, they were polygonal in shape with cytoplasmic protrusions extending in all directions. By 48 hrs, the adherent cells were becoming elongated on all the surfaces. Outcomes showed that the cells attached and spread on each of the Ti surfaces (ungrafted and grafted) in a similar way to that seen on the control Permanox surface that is designed for that purpose. This demonstrated that the Ti surfaces had no negative impact on initial cell adhesion and spreading behavior of the cells during the first 48 hours of direct contact.

3.2.2. Cell proliferation—Cell proliferation on the grafted and ungrafted Ti surfaces was measured using the MTT ((3-(4,5-dimethylthiazol-2-yl)-2,5-diphenyltetrazolium bromide) tetrazolium) assay conducted over 7 days with timepoints at days 1, 4 and 7. Images (see Figure 5) were taken at each timepoint to see if the cells that had attached to the surface of wells around each wafer were affected by presence of wafers (*i.e.*, indirect cytotoxicity check). An additional wafer for each surface was stained with cell tracker green (CTG) on day 7 to check cell morphology and distribution/coverage of cells on the surfaces.

Cell proliferation data over 7 days (Figure 6) showed that the cells on both the grafted and ungrafted Ti surfaces supported steady proliferation over the 7-day period of the assay to equivalent levels, with a slight increase observed on Ti-UV grafted surface at day 7. Although all Ti samples exhibited less cell proliferation than TCPS, this was not unexpected since TCPS is designed to promote cells adhesion and growth. Representative images of CTG stained cells on each of the surfaces on day 7 (Figure 7) confirmed the distribution and vitality of the cells growing on each of the Ti surfaces was similar to that seen on TCPS surface. This outcome was consistent with expectations based on data from the initial cell adhesion assay (as shown in Figure 3). Images of cells attached and spread on the surface of the TCPS wells around the Ti samples (Figure 7) served to further confirm that none of Ti surfaces surface was eluting anything cytotoxic into the cell culture medium during the 7-day period of the proliferation assay.

3.2.3. Cell differentiation and mineralization at day 25—Differentiation of cells was evaluated using assays[35,36] to measure the production of alkaline phosphatase (ALP) (Figure 8) and calcium (Figure 9) in cells adherent to each surface that had been maintained under two different culture regimes (standard and osteogenic) for 25 days. ALP is regarded as a marker for early stage of cell differentiation during the initial phase of extracellular matrix formation. Calcium is a marker for the later stage of cell differentiation where mineralization occurs in the extracellular matrix. In parallel, an MTT assay (Figure 10) conducted in parallel with the differentiation assay (Figure 10) was conducted on day 25 to evaluate cell numbers on each of the surfaces so that ALP and calcium data to be adjusted for the number of cells that were attached to each surface. CTG staining showed that cell coverage for all samples was similar in the undifferentiated and differentiated sample sets. Cells on TCPS were fully confluent and cell cover on Ti control samples was patchy as cells had washed off during handling. Each of the 3 grafted surfaces supported complete cell cover similar to TCPS in the undifferentiated set, with some small uncovered patches evident in the differentiated set.

Outcomes of ALP and calcium assays (Figures 8 **and** 9) corrected for cell number showed that culturing cells under osteogenic conditions promoted the production of both ALP and calcium by the cells compared to that produced by cells maintained on standard culture conditions over the 25-day period of the assay. Cells growing under osteogenic conditions for 25 days on all of the Ti surfaces produced more ALP and calcium than those on TCPS. This was not unusual as TCPS is designed specifically for cell adhesion and spreading, not for differentiation. Cells growing on the ungrafted Ti and the grafted Ti-PR (≈5 kDa) surface produced significantly more ALP than those on the Ti-UV and Ti-TH grafted surfaces when maintained under osteogenic conditions for 25 days (Figure 7). Cells growing on all of the Ti surfaces produced high levels of calcium when maintained under osteogenic conditions, especially the Ti-PR surface (Figure 8).

Together, these outcomes showed that cells adherent to the Ti-UV and Ti-TH grafted surfaces were producing a considerable level of mineral at day 25 indicative of a later stage of differentiation (i.e., the phase where ALP production decreases with a concurrent increase in mineral production as measured by calcium levels). Cells adherent to the Ti-PR grafted surfaces responded differently as they had produced similar levels of ALP to the ungrafted

Ti control, but more Ca compared to Ti control, over the 25-day time period. The relatively high levels of both ALP and Ca produced by cells on the Ti-PR grafted surfaces indicated that some of the cell population was well differentiated and producing mineral while other cells in the cell population were still in an earlier stage of differentiation.

Taken together, Ca and ALP data showed that the cells adherent to UV and TH grafted surfaces had differentiated and were forming mineral by day 25 while the cells on the PR grafted surfaces were producing considerable mineral but had not yet reached their full differentiation state. This means that while all grafted surfaces supported differentiation of Saos2 cells, the UV and TH grafted surfaces induced cell differentiation/mineralization earlier than the PR grafted surface.

3.3. Bacteria adhesion - analysis

For more than twenty years Migonney et *al.*[26,37] showed that the presence of sulfonate groups on any polymer or metallic surface endowed it with anti-bacterial adhesion properties *in vitro* and *in vivo*. Moreover, it was demonstrated that the origin of this activity is due to the affinity and conformation of Fn when adsorbed on the polyNaSS functionalized surfaces in comparison to non-functionalized ones. Recent studies showed that Ti surfaces functionalized by polyNaSS were also capable of inhibiting *S. epidermidis (SE)*[37] and *S. aureus* (SA)[18] adhesion and that the inhibition is mediated and modulated by the presence of Fn (SA) and/or Fg (SE). The inhibiting properties were related to the presence of sulfonate groups on one hand and to the presence of the adhesive proteins at the surface in the "appropriate" conformation on the other hand. For that reason, *S. aureus* adhesion was studied on the different polyNaSS grafted and ungrafted Ti surfaces preadsorbed with pure (Fn) and mixtures of proteins (PPP, dPPP, dPPP+Fn) with the aim of highlighting the role of the pre-adsorbed Fn in the presence of the plasma proteins (PPP, dPPP+Fn) on polyNaSS grafted surfaces on the inhibition of bacteria adhesion as well as the role of the distribution of sulfonate groups and length of polyNaSS macromolecular chains on the grafted Ti surfaces.

The results are all expressed as inhibition percentage (%) of *S. Aureus* bacteria adhesion by polyNaSS surfaces compared to ungrafted Ti samples previously adsorbed with (a) a mixture of proteins (PPP), (b) pure albumin HSA, (c) pure Fn, (d) Fn depleted plasma dPPP and (e) Fn added to depleted plasma dPPP+Fn in Figure 11 for conditions (a), (b) and (c) and in Figure 12 for conditions (d) and (e). All the concentrations of the pre-adsorption assays were set to 10% of the plasma protein concentrations. Results show that:

a. In the presence of plasma proteins (PPP) on the surface (mimicking the proteins mixture under physiologic conditions) the poly(NaSS) grafted surfaces induce an important inhibition of MRSA clinical strain adhesion regardless of the grafting method which varies from 36 to 75%. The highest inhibition value was obtained for the UV grafted surfaces and the lowest for the 5kD grafted surfaces. UV and thermal grafting produced similar results (75% for UV compared to 70% for thermal grafting), confirming that the distribution and availability of sulfonate groups from those grafted polyNaSS chains are similar in both cases. This is not surprising since the polymerization initiated "from" the surface follows the same

radical polymerization process. In addition, these results are consistent with those obtained by Felgueiras et al. for thermal polyNaSS grafting from Ti samples. When analyzing the results obtained on the architecture controlled polyNaSS grafted surfaces, it showed that the inhibition properties depend on the length of the polyNaSS chains more than on their distribution on the surface. Then, even if the coverage of the surfaces by polyNaSS chains is lower “grafting to” than UV and thermal grafting (TB assays and XPS results), the “grafted to” polyNaSS chains, and more precisely the available sulfonate groups, are sufficient in amount and efficiency to provide inhibition rates up to 65% (polyNaSS chains of 35kD). The higher the molecular weight the higher the inhibition rate. Those results are obtained when surfaces are preadsorbed with plasma proteins at 10% (i.e., in the presence of Fn (20 microg/mL) along with the other proteins present in plasma).

b. When plasma proteins from PPP are replaced by Alb (at 10% of its plasma concentration) the rates of inhibition are significantly lowered. HSA is known to cover and passivate all the surfaces with the same affinity. It has no activity on bacteria adhesion except decreasing its access to the surface without any specificity. The inhibition rates are lowered by a factor of 1.5 to 3.3, depending on the surface. The most important result is that when Fn is not present the effect on bacteria adhesion inhibition is significantly lowered.[18]

c. When polyNaSS grafted surfaces are preadosrbed with pure Fn, the inhibition rates of SA adhesion are similar as those obtained in the presence of PPP and higher than in the presence of Alb. This confirms that the presence of Fn, either pure or in a mixture, on the surface of polyNaSS grafted surfaces is able to induce inhibition rates up to 70%. This is consistent with previous results obtained with functionalized PMMA based copolymers, silicone and Ti surfaces.[25] The specificity of the interactions between Fn and polyNaSS grafted surfaces is sufficient to act in pure or mixture conditions, the presence of the other proteins even at higher concentrations does not alter the activity of the bioactive surface; this proves the specificity of the interactions between polyNaSS grafted surfaces/Fn/SA.

d. In the presence of PPP depleted in Fg and Fn, the inhibition rate of bacteria adhesion are similar to those obtained in the presence of pure HSA. This is expected since HSA is the most abundant plasma protein and dPPP still contains HSA but not Fn.

e. In the presence of dPPP + Fn, the inhibition rates recover the values obtained in the presence of pure Fn and or PPP. This is consistent with the role of Fn in the inhibition process of SA adhesion on polyNaSS grafted surfaces. Moreover, the rates are equivalent to those observed in the presence of plasma proteins from PPP. In addition, the effect of the length of polyNaSS chains on the inhibition rate is confirmed, showing that the amount and availability of sulfonate groups are a key point for providing inhibition of SA adhesion in the presence of Fn.

All the above results show the positive role of sulfonate groups on the biological response of grafted Ti surfaces regardless the type of grafting.

Concerning the osteoblast cell response, we yet extensively studied the influence of polyNaSS Ti-TH grafted surfaces in the presence of pure or mixed.[25] Here is the first time that we investigate the influence of the grafted polymer architecture Ti-TH and Ti-UV against Ti-PR. The global cell response shows that the architecture of the grafted polyNaSS chains may influence the osteoblast differentiation with the “grafting to” technique inducing a lower grafting rate and but producing highly efficient polyNaSS chains.

f. The study of the bacteria response demonstrate the synergic role of polyNaSS and adsorbed Fn on the inhibition of bacteria adhesion Nevertheless, by studying more closely the relationship between the inhibition properties of bacteria adhesion and the surface chemistry as well as the polyNaSS architecture and distribution it is interesting to note that the inhibition percentage shows a strong correlation with the XPS atomic % S for these samples. The Ti-TH and Ti-UV samples present the highest inhibition percentages and the highest S whereas for the Ti-PR samples we observed an increase in the inhibition rate while increasing the polyNaSS length or the S content. It is worth noting that in the case of the 35kDa Ti-PR grafted surface the inhibition rate equals that of Ti-TH and Ti-UV samples. S content is a more determinant parameter that the coverage of the surface since even exhibiting a weak and homogeneous distribution over the entire surface 35kDa Ti-PR reach the same inhibition rate as Ti-TH and Ti-UV reach. It means that when the grafting is concentrated at certain points it needs to developed enough sulfonate groups (length) to reach the same activity.

The inhibition of bacteria adhesion of polyNaSS grafted surfaces correlates with the polyNaSS surface concentration more than their distribution. Regardless of the grafted surfaces the observed activity on *SA* adhesion results from specific interactions between adsorbed Fn and the SO_3^- groups distributed on the Ti surfaces resulting in controlled Fn conformation.[25,38]

In Figure 13, it can be observed that fluorescent labeled *S.* Aureus adheres differently on the different polyNaSS grafted and ungrafted surfaces. Regardless of the grafting method, the inhibiting activity of the polymer is verified. The “grafting from” method seems to endow the surface with better inhibiting properties due to a higher coverage of the Ti surface by polyNaSS. However, the “grafting to” functionalized surfaces exhibit an increased bacterial inhibition with the length of the grafted polymer, with the 35kDa sample producing an image that is similar to Ti-Th and Ti-UV images.

4. Conclusions

The aim of this article was to compare the influence of the structure and architecture of a bioactive polyNaSS polymer to the biological response when grafted on Ti surfaces. The “grafting from” technique is compared to “grafting to” technique for both cell and bacteria responses.

The “grafting from” gives dense and homogeneous polyNaSS grafted surfaces for both thermal or UV initiation processes while “grafting to” technique endows surfaces Ti with Ti Ti-UV Ti-TH Ti-PR 5 kDa Ti-PR 10 kDa Ti-PR 35 kDa polyNaSS chains of precise molecular weight (5, 10 and 35 kDa). In both cases, the grafted polyNaSS bioactive polymer is covalently attached to the Ti surface. The biological responses varied with the grafting method.

Assays using mammalian cells showed no evidence of cytotoxicity when cells were in direct contact with any of the Ti grafted surfaces or the ungrafted Ti control. All the grafted surfaces supported similar levels of cell adhesion, spreading and growth/proliferation but there were notable differences between the three grafted surfaces in the cell differentiation assay. Taken together data shows that the “grafted to” Ti-PR method can have an impact on cellular activities but it needs further optimization of the RAFT-based grafting technique to reach its full potential.

Concerning the bacterial response, all grafting conditions had a positive the effect on *S. aureus* (*S. aureus* inhibition). The “grafting from” technique exhibited better inhibition responses against bacteria adhesion than the “grafting to” technique. However, the molecular weight of the “grafted to” polyNaSS influenced the bacteria adhesion response: the higher the molecular weight of grafted polyNaSS the higher the inhibition properties. This relationship between polyNaSS molecular weight and bacterial inhibition involves the difference in Fn molecules adsorbed onto Ti-PR grafted surfaces.

To conclude, the precision RAFT-based “grafting to” technique showed promising outcomes when tested using osteoblast cell activity and S. aureus adhesion with increased levels of bacterial inhibition as the molecular weight of polyNaSS increased.

Comparison of the new “grafting to” technique with previously tested “grafted from” techniques using thermal and UV irradiation revealed subtle differences in the cell response. We propose that optimizing the RAFT-based “grafting to” technique is needed to fully demonstrate the utility of this precision technique for the purpose of improving long-term outcomes for orthopedic implants.

Acknowledgments

This research was supported by the French Ministry of National Education, Higher Education and Research. The XPS and ToF-SIMS experiments done at NESAC/BIO were supported by NIH grant EB-002027. We especially thank Gerry Hammer (NESAC/BIO) for his help with the XPS analysis and Dr. Dan Graham (NESAC/BIO) for his help with the ToF-SIMS analysis.

References

1. Niinomi M. Mechanical biocompatibilities of titanium alloys for biomedical applications. J. Mech. Behav. Biomed. Mater. 2008; 1:30–42. [PubMed: 19627769]
2. Niinomi M. Recent metallic materials for biomedical applications. Metall. Mater. Trans. A. 2002; 33A:477–486.
3. Long M, Rack HJ. Titanium alloys in total joint replacement: a materials science perspective. Biomaterials. 1998; 19:1621–1639. [PubMed: 9839998]

4. Klabunde Windler, M. Titanium in medicine. Brunette, DMT.Tengvall, P.Textor, M., Thomsen, P., editors. Berlin: Springer; 2001. p. 703
5. Michiardi A, Hélary G, Nguyen PCT, Gamble LJ, Anagnostou F, Castner DG, Migonney V. Bioactive polymer grafting onto titanium alloy surfaces. Acta Biomater. 2010; 6:647–675.
6. Schwartz Z, Avaltroni MJ, Danahy MP, Silverman BM, Hanson EL, Schwarzbauerb JE, Midwoodb KS, Gawalt ES. Cell attachment and spreading on metal implant materials. Mater. Sci. Eng. C. 2003; 23:395–400.
7. Puleo A, Nanci A. Understanding and controlling the bone-implant interface. Biomaterials. 1999; 20:2311–2321. [PubMed: 10614937]
8. Liu X, Chu PK, Ding C. Surface modification of titanium, titanium alloys, and related materials for biomedical applications. Mater. Sci. Eng. R. 2004; 47:49–121.
9. Le Guéhennec L, Soueidan A, Layrolle P, Amouriq Y. Surface treatments of titanium dental implants for rapid osseointegration. Dent. Mater. 2007; 23:844–854. [PubMed: 16904738]
10. Puleo DA, Nanci A. Understanding and controlling the bone implant interface. Biomaterials. 1999; 20:2311–2321. [PubMed: 10614937]
11. Bachle M, Kohal RJ. A systematic review of the influence of different titanium surfaces on proliferation, differentiation and protein synthesis of osteoblast-like MG63 cells. Clin. Oral Implants Res. 2004; 15:683–920. [PubMed: 15533129]
12. Meyer U, Buchter A, Wiesmann HP, Joos U, Jones DB. Basic reactions of osteoblasts on structured material surfaces. Eur. Cell. Mater. 2005; 9:39–49. [PubMed: 15852237]
13. Yoshinari M, Oda Y, Kato T, Okuda K, Hirayama A. Influence of surface modifications to titanium on oral bacterial adhesion in vitro. J. Biomed. Mater. Res. 2000; 52:388–394. [PubMed: 10951380]
14. Cen L, Neoh KG, Kang ET. Antibacterial activity of cloth functionalized with N-alkylated poly(4-vinylpyridine). J. Biomed. Mater. Res. A. 2004; 71:70–80. [PubMed: 15368256]
15. Tiller JC, Liao CJ, Lewis K, Klibanov AM. Designing surfaces that kill bacteria on contact. Proc. Natl. Acad. Sci. USA. 2001; 98:5981–5985. [PubMed: 11353851]
16. Chua PH, Neoh KG, Kang ET, Wang W. Surface functionalization of titanium with hyaluronic acid/chitosan polyelectrolyte multilayers and RGD for promoting osteoblast functions and inhibiting bacterial adhesion. Biomaterials. 2008; 29:1412–1421. [PubMed: 18190959]
17. Delmi M, Vaudaux P, Lew DP, Vasey H. Role of fibronectin in staphylococcal adhesion to metallic surfaces used as models of orthopaedic devices. J. Orthop. Res. 1994; 12:432–438. [PubMed: 8207597]
18. Anagnostou F, Debet A, Pavon-Djavid G, Goudiaby Z, Hélary G, Migonney V. Osteoblast functions on functionalized PMMA-based polymers exhibiting Staphylococcus aureus adhesion inhibition. Biomaterials. 2006; 27(21):3912–3919. [PubMed: 16564569]
19. Berlot S, Aissaoui Z, Pavon-Djavid G, Belleney J, Jozefowicz M, Hélary G, Migonney V. Biomimetic poly(methyl methacrylate)-based terpolymers: modulation of bacterial adhesion effect. Biomacromolecules. 2002; 3:63–68. [PubMed: 11866557]
20. Crémieux AC, Pavon-Djavid G, Saleh Mghir A, Hélary G, Migonney V. Bioactive polymers grafted on silicone to prevent Staphylococcus aureus prosthesis adherence: *in vitro* and *in vivo* studies. JABBS. 2003; 1:178–185.
21. Harris LG, Tosatti S, Wieland M, Textor M, Richards RG. *Staphylococcus aureus* adhesion to titanium oxide surfaces coated with non-functionalized and peptide-functionalized poly(L-lysine)-grafted-poly(ethylene glycol) copolymers. Biomaterials. 2004; 25:4135–4148. [PubMed: 15046904]
22. Norowski PA Jr, Bumgardner JD. Biomaterial and antibiotic strategies for periimplantitis: a review. J. Biomed. Mater. Res. B. Appl. Biomater. 2009; 88:530–543. [PubMed: 18698626]
23. Wan T, Aoki H, Hikawa J, Lee JH. RF-magnetron sputtering technique for producing hydroxyapatite coating film on various substrates. Biomed. Mater. Eng. 2007; 17:291–297. [PubMed: 17851171]
24. El Khadali F, Hélary G, Pavon-Djavid G, Migonney V. Modulating fibroblast cell proliferation with functionalized poly(methyl methacrylate)-based copolymers: chemical composition and monomer distribution effect. Biomacromolecules. 2002; 3:51–56. [PubMed: 11866555]

25. Latz C, Pavon-Djavid G, Hélary G, Evans MDM, Migonney V. Alternative intracellular signaling mechanism involved in the inhibitory biological response of functionalized PMMA-based polymers. Biomacromolecules. 2003; 4:766–771. [PubMed: 12741796]
26. Felgueiras HP, Ben Aissa I, Evans MDM, Migonney V. Contributions of adhesive proteins to the cellular and bacterial response to surfaces treated with bioactive polymers: case of poly(sodium styrene sulfonate) grafted titanium surfaces. J. Mater. Sci.: Mater. Med. 2015; 26:261. [PubMed: 26449451]
27. Alcheikh A, Pavon-Djavid G, Hélary G, Petite H, Migonney V, Anagnostou F. PolyNaSS grafting on titanium surfaces enhances osteoblast differentiation and inhibits *Staphylococcus aureus* adhesion. J. Mater. Sci.: Mater. Med. 2013; 24:1745–1754. [PubMed: 23625318]
28. Felgueiras HP, Decambron A, Manassero M, Tulasne L, Evans MDM, Viateau V, Migonney V. Bone tissue response induced by bioactive polymer functionalized Ti6Al4V surfaces: *In vitro* and *in vivo* study. J. Colloid Interface Sci. 2017; 491:44–54. [PubMed: 28012912]
29. Hélary G, Noirclère F, Mayingi J, Migonney V. A new approach to graft bioactive polymer on titanium implants: Improvement of MG 63 cell differentiation onto this coating. Acta Biomaterialia. 2009; 5:124–133. [PubMed: 18809363]
30. Chouirfa H, Migonney V, Falentin-Daudré C. Grafting bioactive polymers onto titanium implants by UV irradiation. RSC Advances. 2016; 6:13566–13771.
31. Falentin-Daudré C, Migonney V, Chouirfa H, Baumann JS. Process for grafting bioactive polymers onto metallic materials PCT/EP2016/068909.
32. Chouirfa H, Evans MDM, Castner DG, Bean P, Mercier D, Galtayries A, Falentin-Daudré C, Migonney V. Grafting of architecture controlled poly(styrene sodium sulfonate) onto titanium surfaces using bio-adhesive molecules: Surface and biological properties. Biointerphases. 2017; 12(2)
33. Sano S, Kato K, Ikada Y. Introduction of functional groups onto the surface of polyethylene for protein immobilization. Biomaterials. 1993; 14(11):817–822. [PubMed: 8218735]
34. Kato K, Ikada Y. Selective adsorption of proteins to their ligands covalently immobilized onto microfibers. Biotechnology and Bioengineering. 1995; 47:557–566. [PubMed: 18623435]
35. Prideaux M, Wijenayaka AR, Kumarasinghe DD. Saos-2 Osteosarcoma cells as an in vitro model for studying the transition of human osteoblasts to osteocytes. Calcif. Tissue Int. 2014; 95:183–193. [PubMed: 24916279]
36. Czekanska EM, Stoddart MJ, Ralphs JR, Richards RG, Hayes JS. A phenotypic comparison of osteoblast cell lines versus human primary osteoblasts for biomaterials testing. J. Biomed. Mater. Res. A. 2014; 102:2636–2643. [PubMed: 23983015]
37. Vasconcelos DM, Falentin-Daudré C, Blanquaert D, Thomas D, Granja PL, Migonney V. Role of protein environment and bioactive polymer grafting in the *S. epidermidis* response to titanium alloy for biomedical applications. Materials Science and Engineering C. 2014; 45(1):176–183. [PubMed: 25491817]
38. An YH, Friedman RJ. Concise review of mechanisms of bacterial adhesion to biomaterial surfaces. J. Biomed. Mater. Res. 1998; 43:338–348. [PubMed: 9730073]

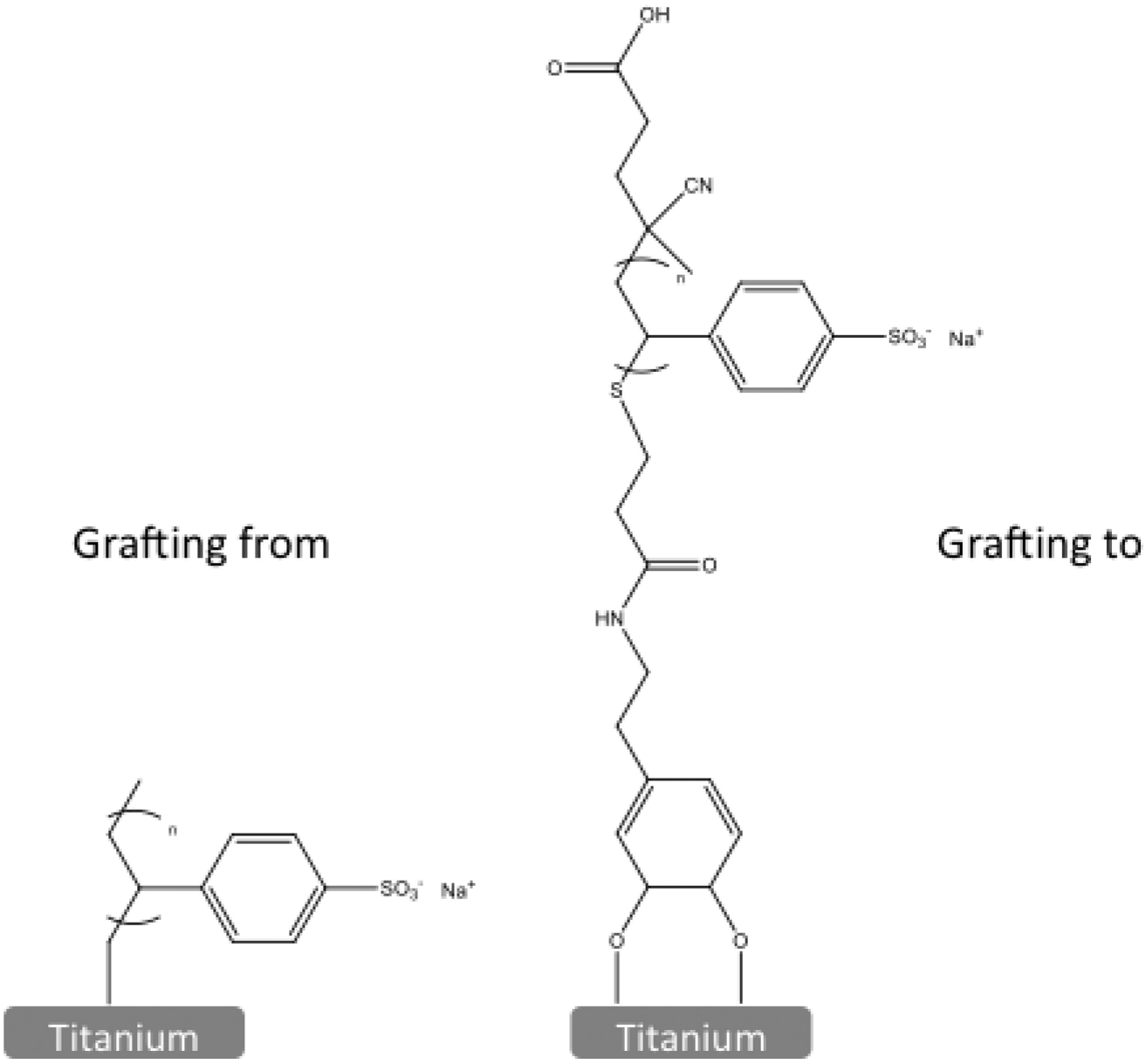

Figure 1.
Representation the grafted polyNaSS surface prepared by “grafting from” (left) and “grafting to” involving a catechol group (right).

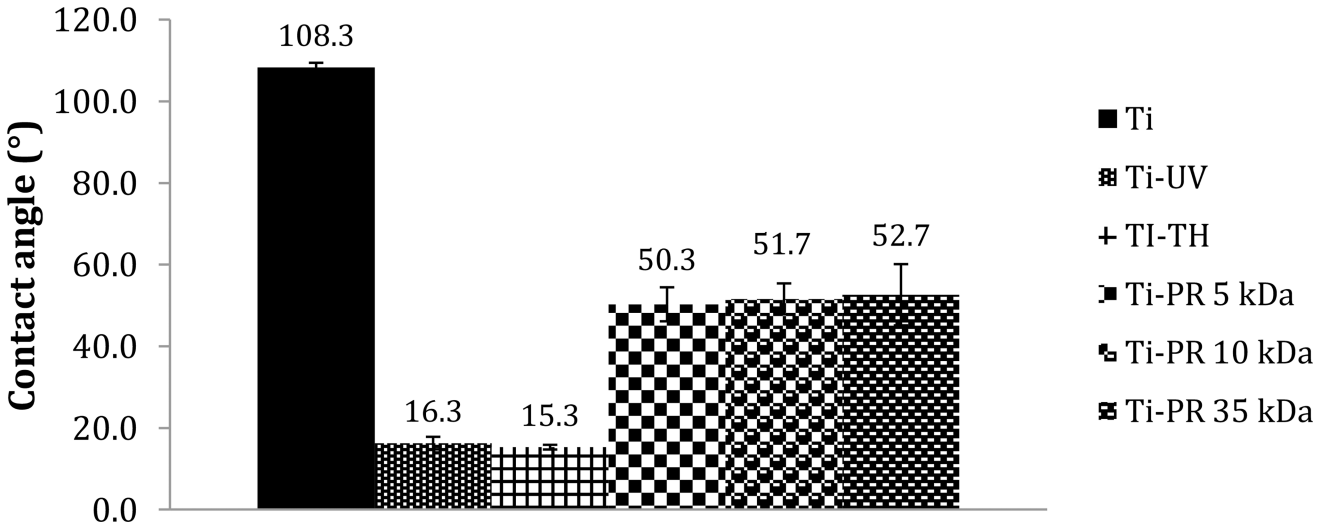

Figure 2.
Contact angle measurements on PolyNaSS grafted and ungrafted samples.

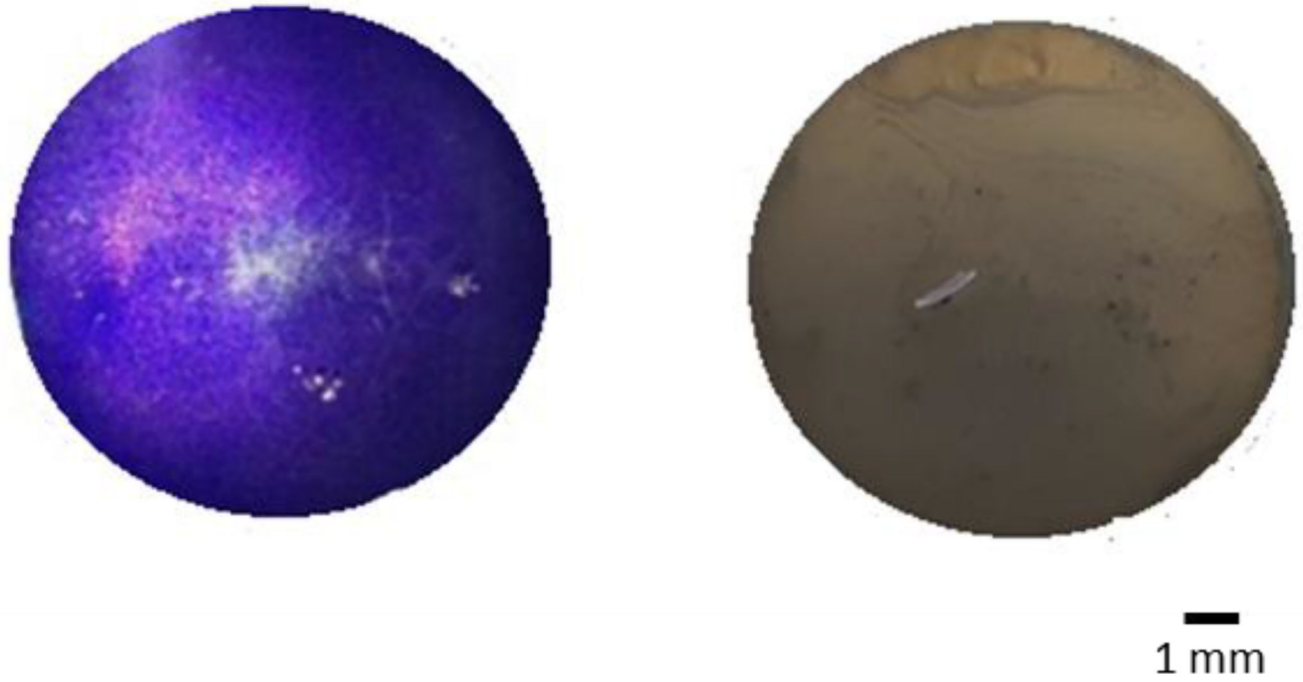

Figure 3.
TB images of polyNaSS grafted Ti surfaces: “grafting from” technique (left) and “grafting to” technique (right).

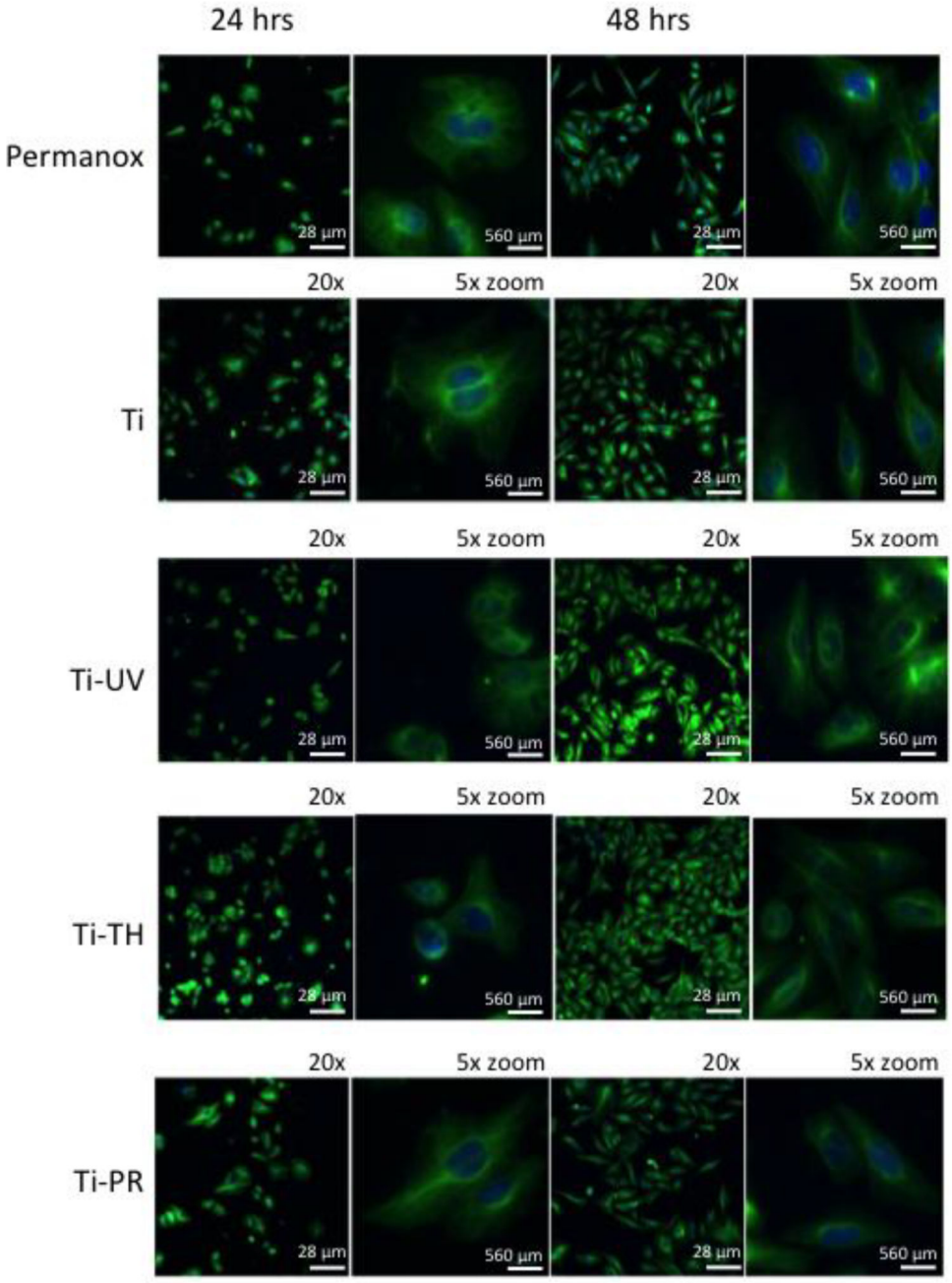

Figure 4.

Representative confocal images of cells attached to control Permanox wells and test Ti wafer surfaces at 24 hrs and 48 hrs (Green tubulin stained cell cytoskeleton with blue DAPI stained for cell nuclei. Images shown at 20× as well as additional 5× zoom).

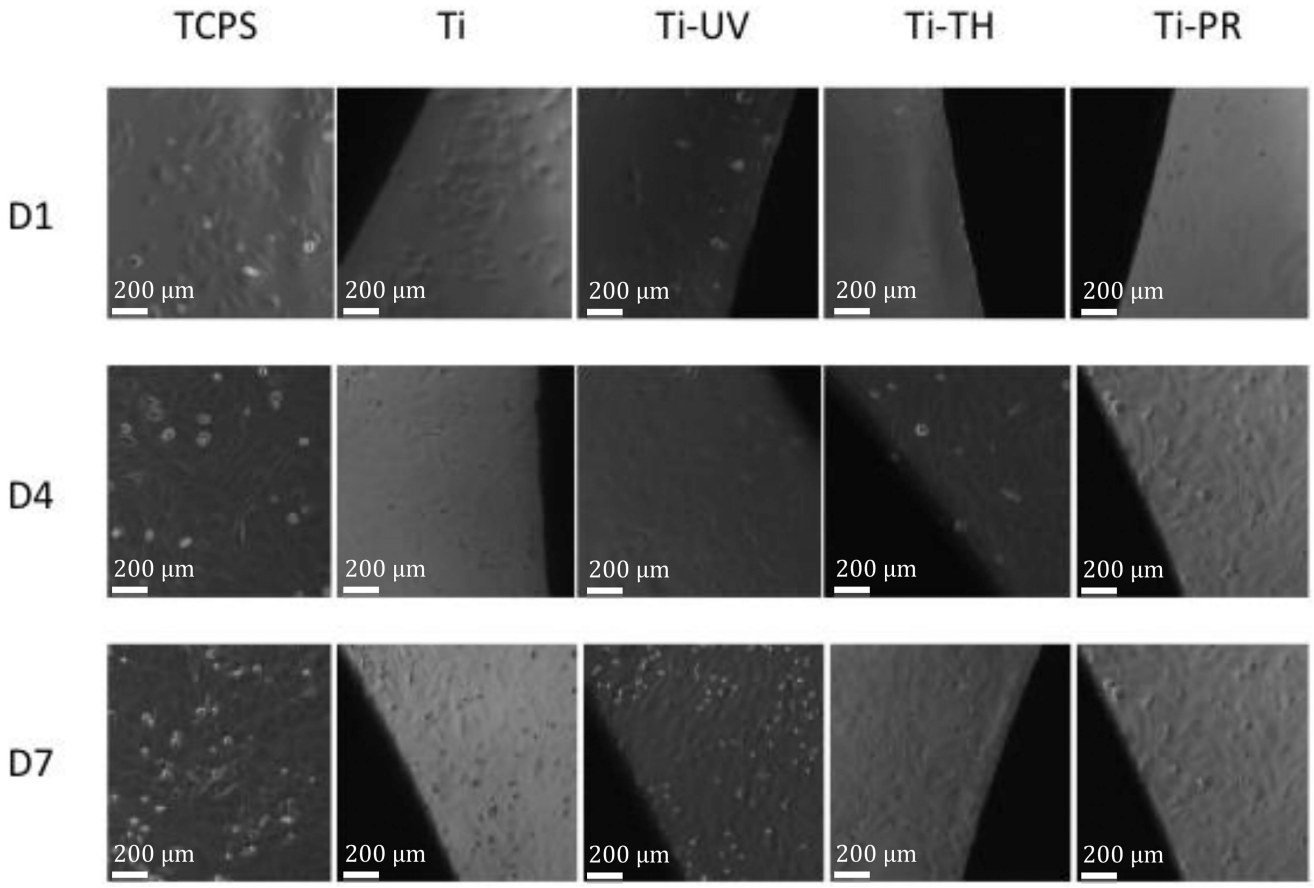

Figure 5.
Phase contrast images taken at Days 1, 4 and 7: attached and spread cells were observed on the control TCPS surfaces as well as on all the test wafers.

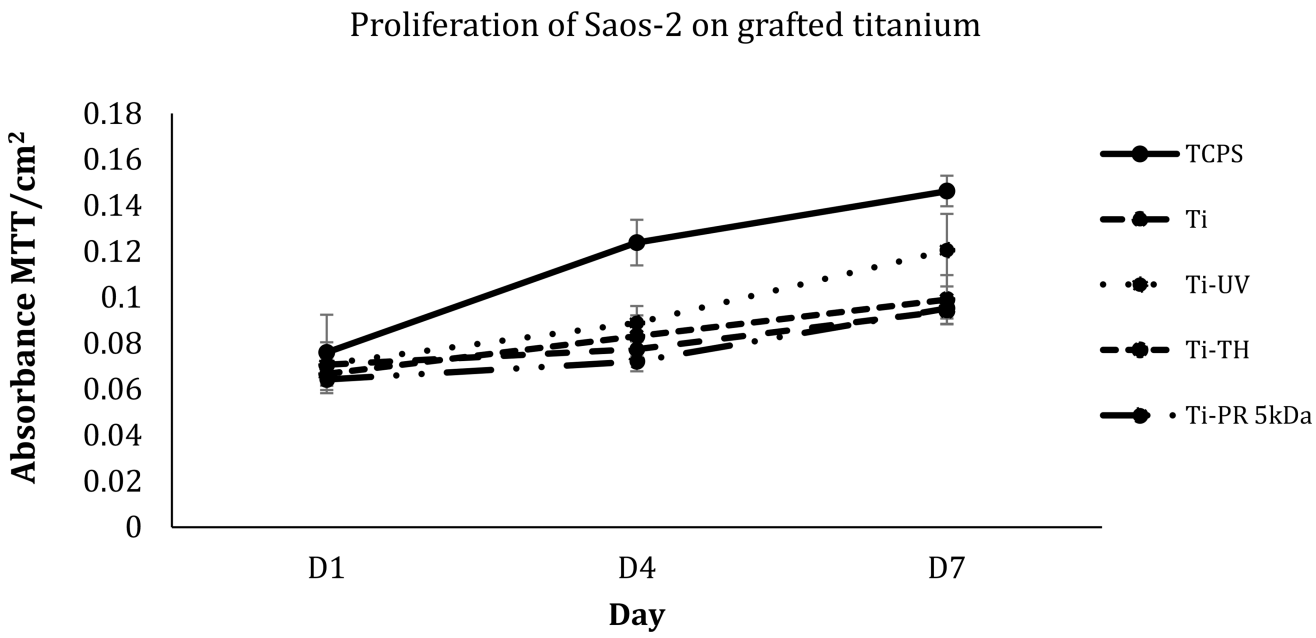

Figure 6.

Proliferation of cells on grafted and ungrafted surfaces measured by MTT assay conducted at timepoints of 1, 4 and 7 days (data is based on triplicate samples of each wafer included at each of the 3 timepoints ±SDM).

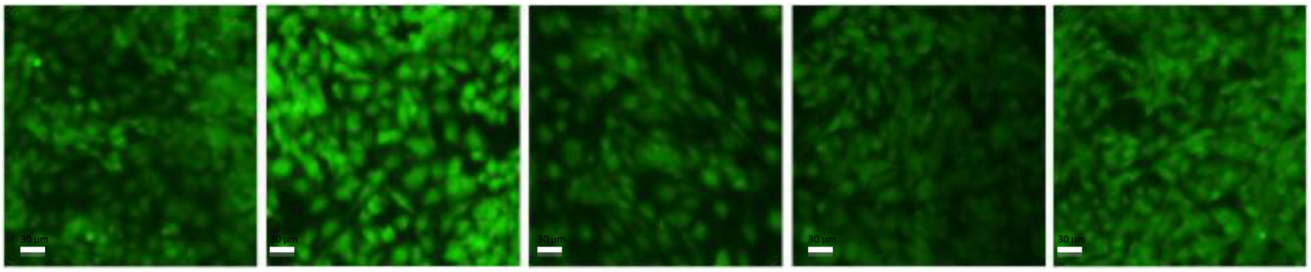

Figure 7.

Representative fluorescent images of adherent cells on control TCPS and test Ti wafers on day 7 of the proliferation assay (CTG green stained cells at 20× magnification).

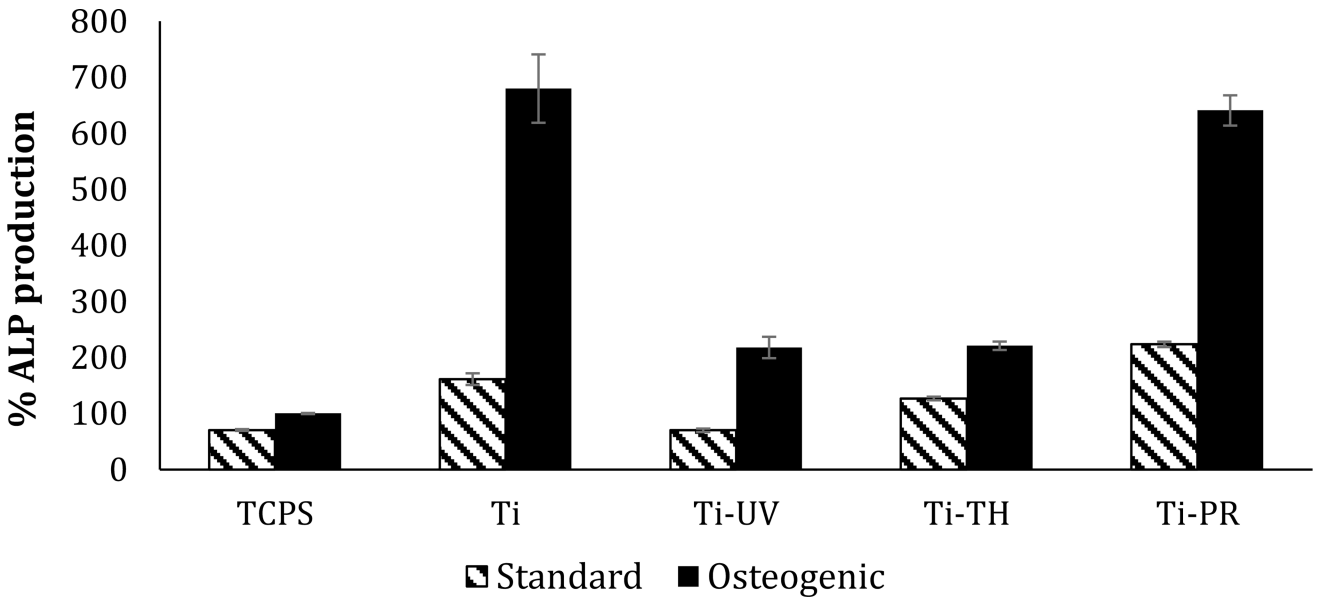

Figure 8.

Alkaline phosphatase (ALP) produced by cells adherent to the control TCPS, grafted and ungrafted Ti surfaces (data represents the mean of triplicate samples of each surface corrected for cell number as measured using MTT assay run in parallel over 25 days and normalized to production by cells on control TCPS under osteogenic conditions ± SDM).

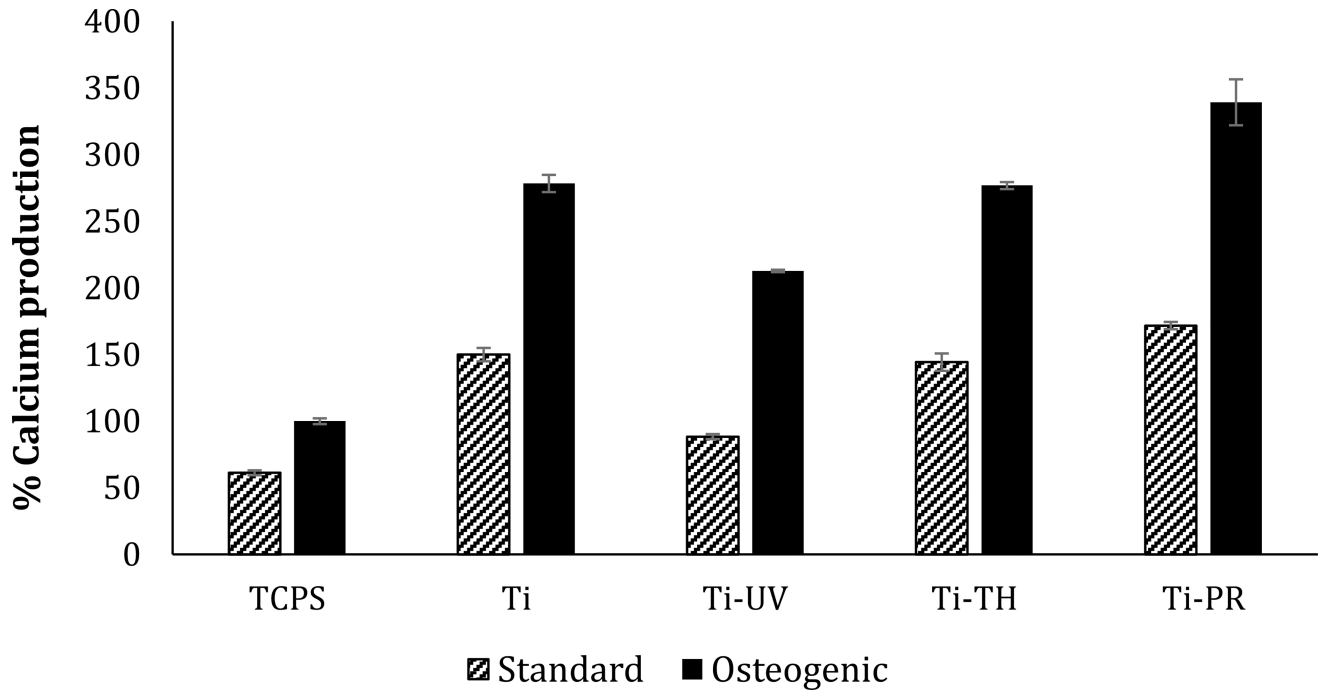

Figure 9.

Calcium produced by cells adherent to the grafted and ungrafted Ti surfaces (data represents the mean of triplicate samples of each surface corrected for cell number as measured using MTT assay run in parallel over 25 days and normalized to production by cells on control TCPS under osteogenic conditions ± SDM).

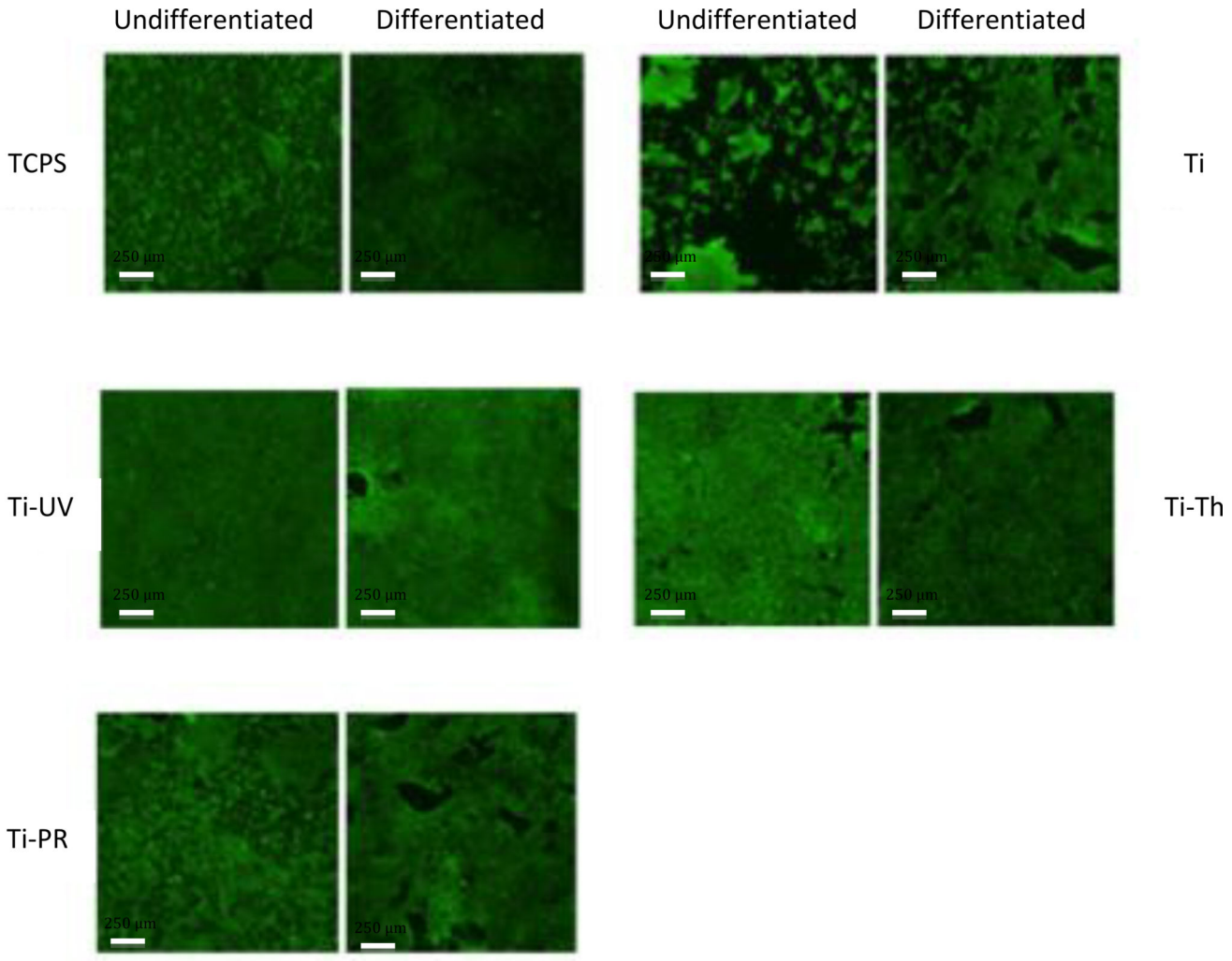

Figure 10.
Cell average on each of the surfaces in undifferentiated and differentiated sets at day 25 of the differentiation assay (cells stained with cell tracker green CTG to visualize them).

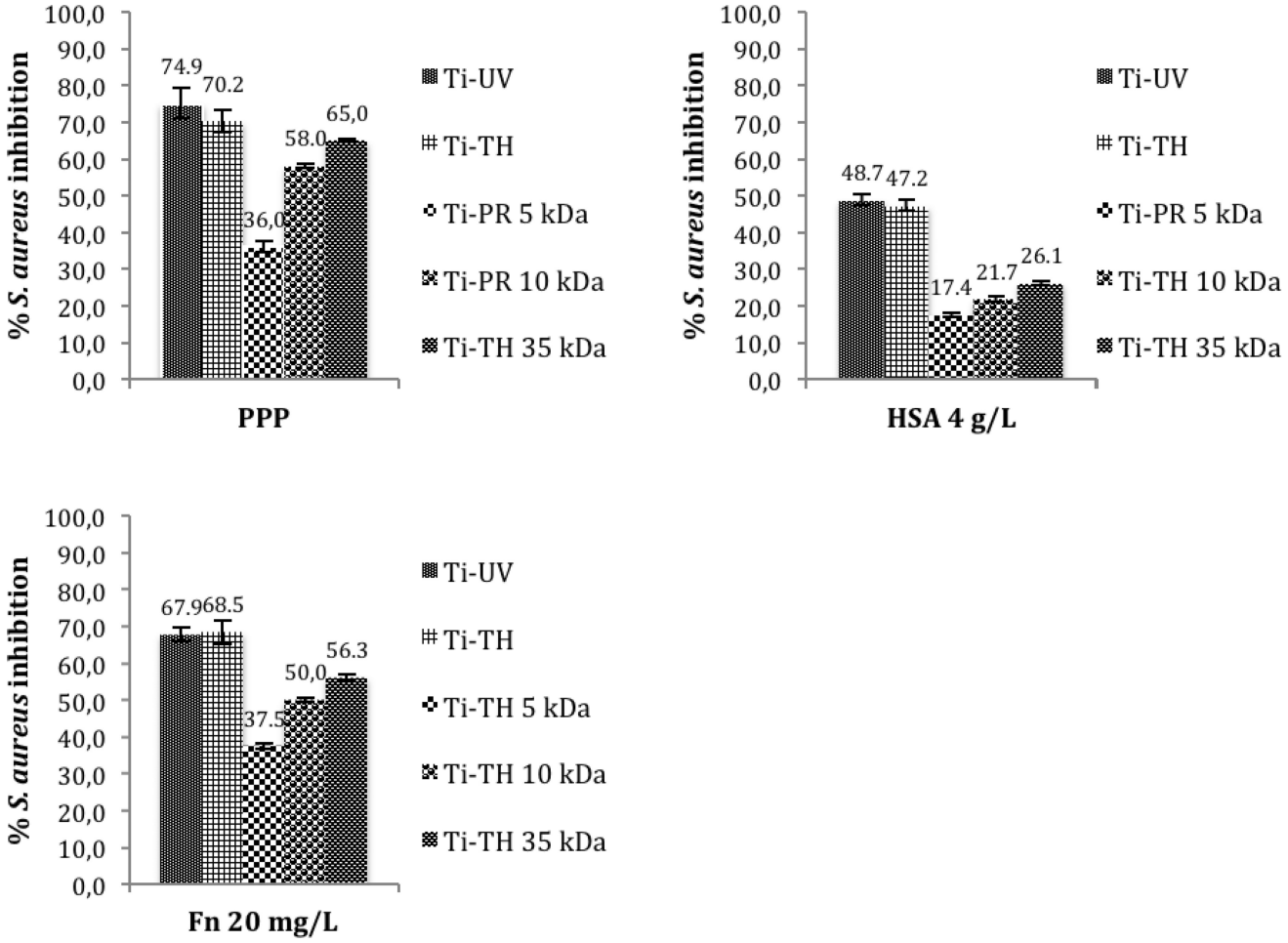

Figure 11.

Inhibition of *S. aureus* adhesion on polyNaSS grafted Ti surfaces previously adsorbed by pure proteins and mixtures (PPP, HSA and Fn) relative to ungrafted surfaces (1 h culture, 37°C).

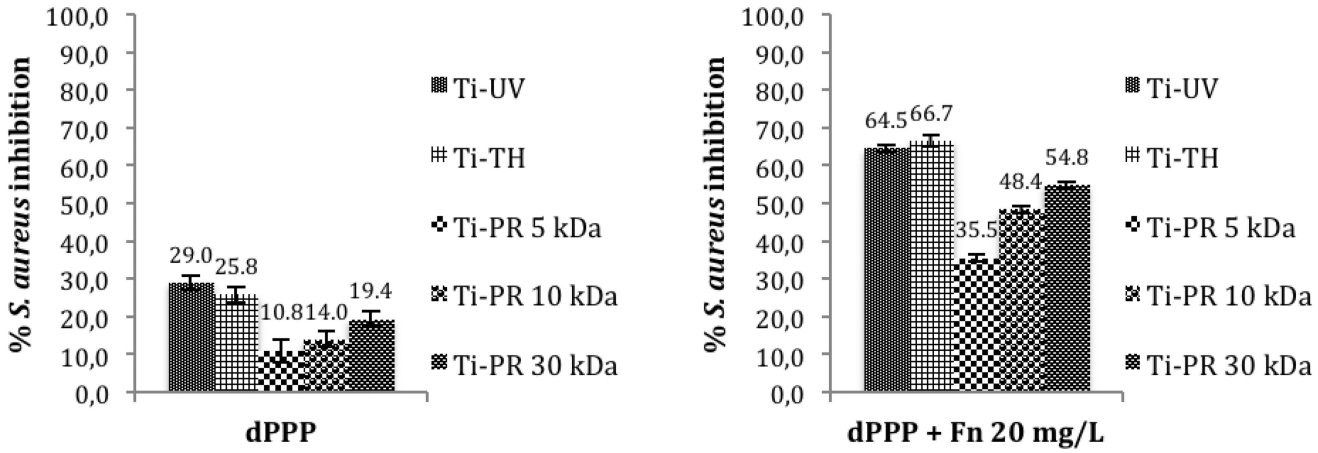

Figure 12.

Inhibition of adhesion of *S. aureus* on grafted Ti surfaces pre-adsorbed with different protein solutions (dPPP and dPPP + Fn 20 mg/mL) relative to ungrafted surfaces (1 h culture, 37°C).

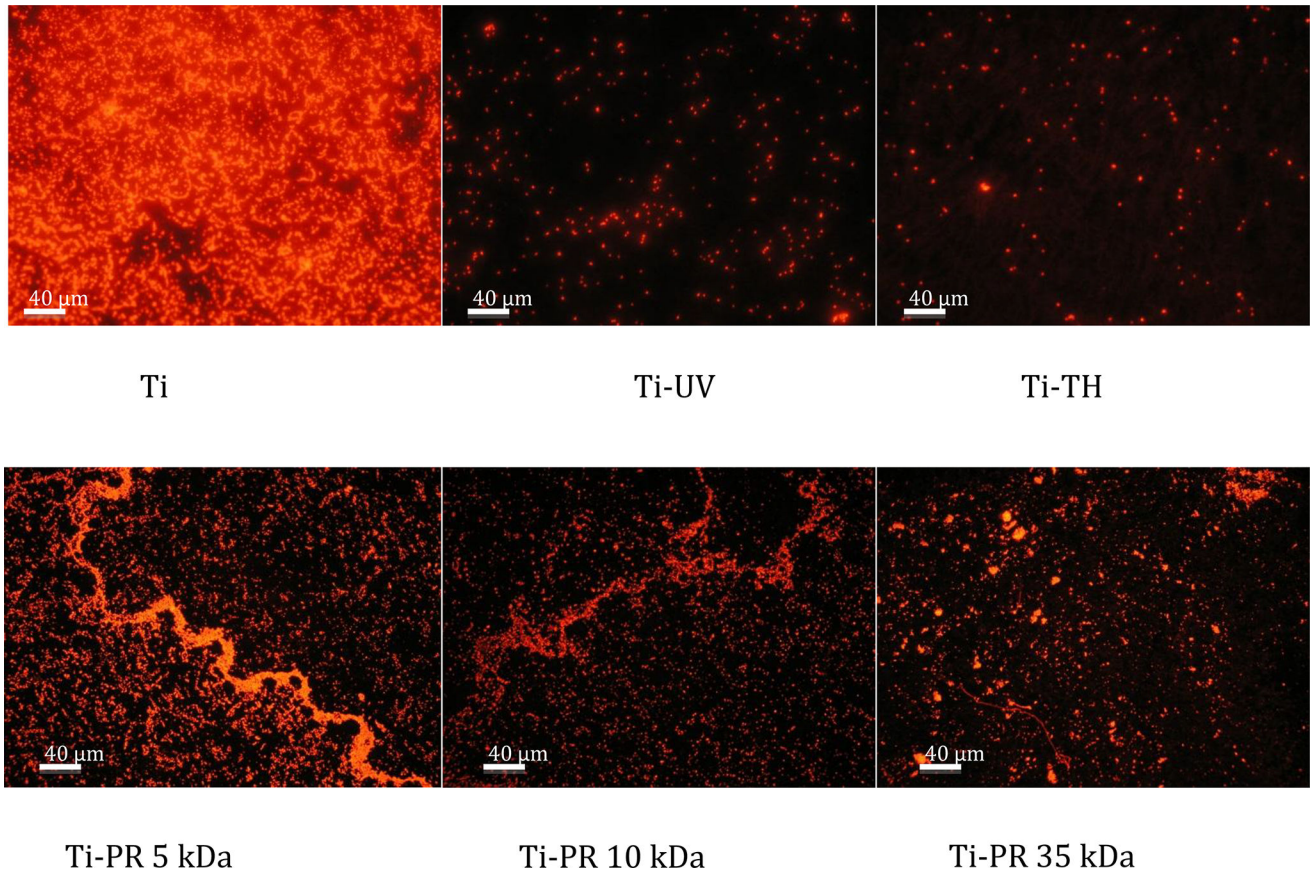

Figure 13.
Fluorescent detection of *S. aureus* on different surfaces preadsorbed with pure plasma for 1 h.

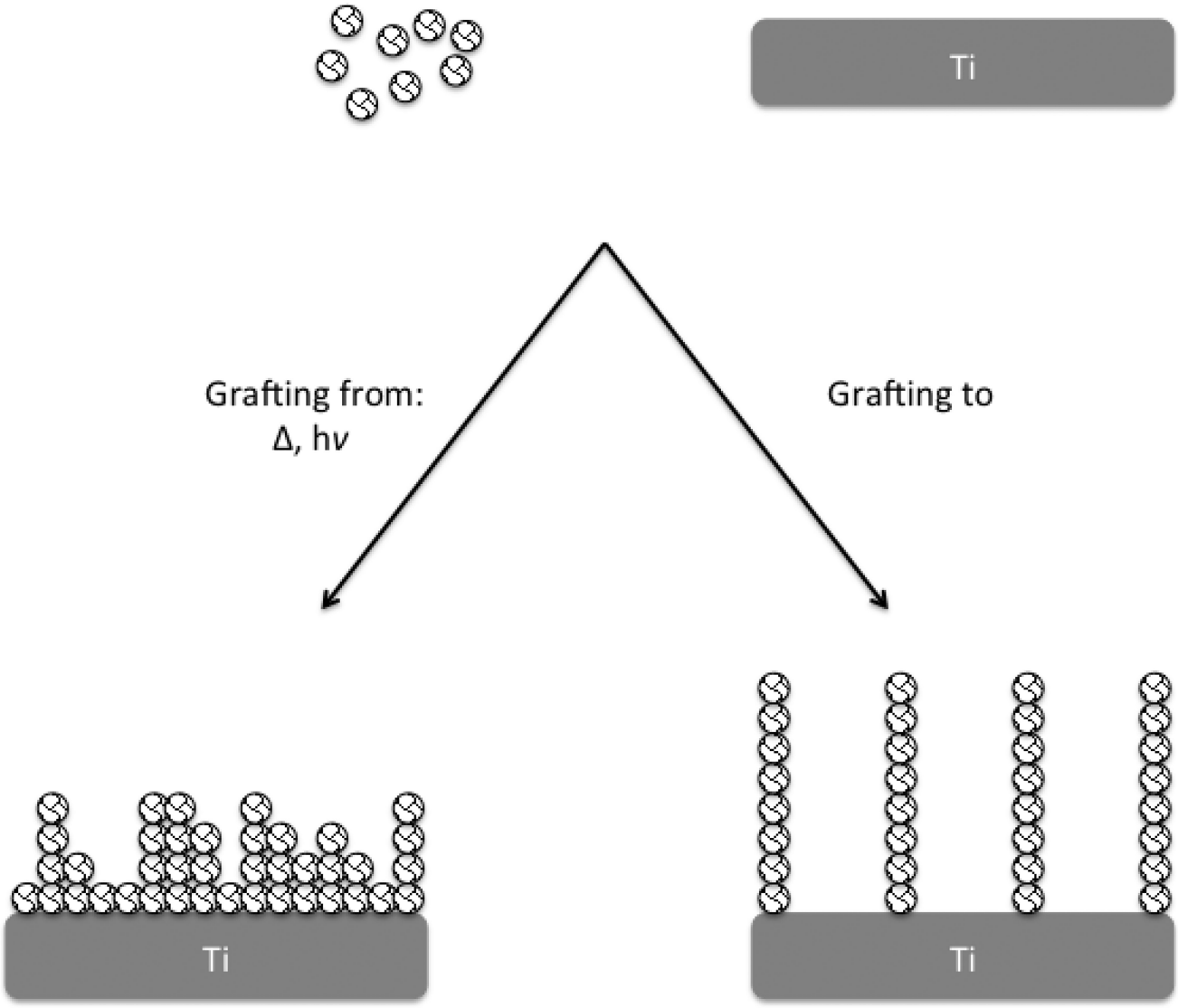

Scheme 1.

The “grafting from” includes thermal polyNaSS grafting (Δ) and UV polyNaSS grafting (h*ν*) and gives a distribution of the polymer chains size whereas the “grafting to” leads to the grafting of polymer chains of precise and unique size.

Table 1

Details of polyNaSS grafted surfaces.

Surface	Details	Reference
Ti Control	Non-grafted	Ti
Thermal grafted Ti	Grafted from	Ti-TH
UV grafted Ti	Grafted from	Ti-UV
Architecture controlled grafted surface	Grafted to	Ti-PR

Table 2

XPS determined surface atomic composition of the “grafted from” (Ti-TH and Ti-UV) and “grafted to” (≈5, ≈10, ≈35 kDa Ti-PR) polyNaSS samples. The number of spots analyzed (n) is also indicated.

	XPS atomic percent						
Samples	**C**	**O**	**Ti**	**N**	**S**	**Na**	**Others**
Ti-TH (n=4)	58.3 ± 5.7	28.2 ± 4.8	2.5 ± 2.3	-	7.0 ± 1,0	2,4 ± 0.4	-
Ti-UV (n=10)	59.6 ± 4.1	27.7 ± 3.4	2.7 ± 2.7	-	6.6 ± 1.4	1.8 ± 0.7	-
Ti-PR (≈5 kDa, n=6)	57.3 ± 4.6	29.3 ± 3.3	7.3 ± 2.5	0.5 ± 0.3	2.8 ± 1.4	2.2 ± 0.4	F
Ti-PR (≈10 kDa, n=6)	55.3 ± 9.3	29.4 ± 3.9	6.7 ± 1.5	1.7 ± 0.4	2.0 ± 0.8	1.8 ± 0.9	F, Zn, Ca
Ti-PR (≈35 kDa, n=6)	64.8 ± 6.7	22.8 ± 4.4	2.8 ± 2.4	0.4 ± 0.2	4.8 ± 1.2	3.2 ± 1.0	Zn

Table 3

TB analysis of the polyNaSS grafting rate as a function of the grafting process: "grafting from" (Ti-TH and Ti-UV) and "grafting to" (Ti-PR 5, 10, 35 kDa).

	Ti-TH	TI-UV	Ti-PR 5 kDa	Ti-PR 10 kDa	Ti-PR 35 kDa
polyNaSS grafting rate (μg/cm^2)	5 ± 0.3	4.4 ± 0.3	0.7 ± 0.1	0.8 ± 0.1	0.8 ± 0.1